Audiovisual Biofeedback Improves CineeMagnetic Resonance Imaging Measured Lung Tumor Motion Consistency

Danny Lee, MSc,* Peter B. Greer, PhD,[y,z] Joanna Ludbrook, FRANZCR,[z] Jameen Arm, MSc,[z] Perry Hunter, BSc,[z] Sean Pollock, MSc,* Kuldeep Makhija, PGDCA,* Ricky T. O'Brien, PhD,* Taeho Kim, PhD,*,[x] and Paul Keall, PhD*

*Radiation Physics Laboratory, Sydney Medical School, The University of Sydney, Sidney, NSW, Australia; [y] School of Mathematical and Physical Sciences, The University of Newcastle, Newcastle, NSW, Australia; [z] Department of Radiation Oncology, Calvary Mater Newcastle, Newcastle, NSW, Australia;

[x] Department of Radiation Oncology, Virginia Commonwealth University, Richmond, Virginia

Corresponding Author: Paul Keall

Paul Keall, PhD, Radiation Physics Laboratory, Sydney Medical School, The University of Sydney, Room 475, Blackburn Building D06, Sidney, NSW 2006, Australia. Tel: (+61) 2-9351-3385; E-mail: paul.keall@sydney.edu.au

Supported by a National Health and Medical Research Council Australia Fellowship.

Conflict of interest: P.K. is an inventor on US patent 7,955,270 related to audiovisual biofeedback. P.K., S.P., R.O., and K.M. are founders of a company (Respiratory Innovations) that has the goal of disseminating a cost-effective breathing guidance solution.

Acknowledgments: the authors thank Julie Baz for reviewing the manuscript for clarity

Summary

Can audiovisual biofeedback improve lung tumor motion consistency throughout medical imaging and radiation therapy procedures? A guiding wave, customized for each patient according to a reference breathing pattern, was used for audiovisual biofeedback across 2 MRI sessions. Lung tumor motion, measured directly from cine-MRI, was significantly more consistent when using audiovisual biofeedback.

Abstract

Purpose

To assess the impact of an audiovisual (AV) biofeedback on intra- and interfraction tumor motion for lung cancer patients.

Methods and Materials

Lung tumor motion was investigated in 9 lung cancer patients who underwent a breathing training session with AV biofeedback before 2 3T magnetic resonance imaging (MRI) sessions. The breathing training session was performed to allow patients to become familiar with AV biofeedback, which uses a guiding wave customized for each patient according to a reference breathing pattern. In the first MRI session (pretreatment), 2-dimensional cine-MR images with (*1*) free breathing (FB) and (*2*) AV biofeedback were obtained, and the second MRI session was repeated within 3-6 weeks (mid-treatment). Lung tumors were directly measured from cine-MR images using an auto-segmentation technique; the centroid and outlier motions of the lung tumors were measured from the segmented tumors. Free breathing and AV biofeedback were compared using several metrics: intra- and interfraction tumor motion consistency in displacement and period, and the outlier motion ratio.

Results

Compared with FB, AV biofeedback improved intrafraction tumor motion consistency by 34% in displacement (P=.019) and by 73% in period (P<.001). Compared with FB, AV biofeedback improved interfraction tumor motion consistency by 42% in displacement (P<.046) and by 74% in period (P=.005). Compared with FB, AV biofeedback reduced the outlier motion ratio by 21% (P<.001).

Conclusions

These results demonstrated that AV biofeedback significantly improved intra- and interfraction lung tumor motion consistency for lung cancer patients. These results demonstrate that AV biofeedback can facilitate consistent tumor motion, which is advantageous toward achieving more accurate medical imaging and radiation therapy procedures.

Introduction

Breathing variations (1-5) can cause image artifacts in 4-dimensional CT images (6) used in radiation therapy treatment planning and lead to a greater variation in tumor motion between treatment planning and treatment delivery (7, 8). In addition, breath-to-breath (intrafraction) variation compromises the quality of radiation delivery, because it causes an averaging or blurring of dose distribution over the path of the tumor motion, whereas day-to-day (interfraction) variations cause a shift of the dose distribution (9).

Breathing management techniques using patient respiratory signals such as respiratory gating (10), training (11), and breath-holds (12) have been developed to address intrafraction breathing variability. However, interfraction variability from the daily changes of patient breathing is still prominent (10, 13), and this variability is larger than intrafraction variability (1 - 3). Tumor motion tracking has also been developed to account for tumor motion variability. This technique can decrease the uncertainty of respiratory-induced tumor motion; however, noninvasive, markerless lung tumor tracking is not in widespread use (14, 15).

Audiovisual (AV) biofeedback (10, 11, 16, 17, 18, 19), an interactive personalized breathing guidance system, has been developed to minimize breathing variability. Audiovisual biofeedback uses an external respiratory signal from a real-time position management (RPM) system (Varian, Palo Alto, CA) to track patient breathing in real-time. Previous AV biofeedback results have demonstrated that the breathing consistency of external and internal surrogates has been improved (10, 11, 16, 17) while maintaining a robust correlation between external and internal breathing motion (20). However, AV biofeedback results on tumor motion have been less conclusive (21, 22), with additional further investigation strongly suggesting that patient compliance and performance with AV biofeedback improve with time (23). In addition, the variation of lung tumor in outlier motion has not been matched to treatment margins.

In this study, we introduced a novel approach of AV biofeedback for non-small cell lung cancer patients, involving a breathing training session to obtain a guiding wave customized for each patient according to a reference breathing pattern with AV biofeedback and using the guiding wave over 2 3T magnetic resonance imaging (MRI) sessions. This study is the first investigation of the impact of AV biofeedback on lung tumor motion consistency, both intra- and interfractionally, directly measured from cine-MR images.

Methods and Materials

Patients

Nine non-small cell lung cancer patients (aged 25-74 years) with a stage varying from I to III of any histology to be treated using radiation therapy were enrolled in an ethics-approved protocol. Excluded patients had the presence of metallic objects such as surgical clips, surgery metalware, and pacemakers. This study was designed with a breathing training session followed by 2 MRI sessions across different dates (pre- and mid-treatment). The breathing training session was scheduled on the same day of the first MRI session, and the second MRI session was then repeated within 3 to 6 weeks at approximately the midpoint of the radiation treatment.

Audiovisual biofeedback

A breathing training session was performed to allow patients to become familiar with a guiding wave; an average of 10 breathing cycles was calculated using a Fourier Series fit (19),

customized in the displacement and period of respiratory cycles (24), and presented to them on the AV biofeedback breathing guide. Figure 1a shows the workflow of operation of AV biofeedback. Patient breathing is tracked in real-time using RPM, which monitors the up (as they inhale) and down (as they exhale) motion of the gray marker-block positioned on the patient's abdomen. The guiding wave is displayed on the patient's visual display in inhale and exhale breathing limits as the gray horizontal lines that frame the blue wave. The patient then adjusts their breathing such that a gray marker-block on their visual display stays within the breathing limits and traces the motion of the guiding wave.

Two experimental setups of AV biofeedback for a breathing training session (Fig. 1b) used a ceiling-mounted RPM and display goggles. For the MRI setup, a mobile RPM and a mirror-display setup overlooking an MR-compatible projection screen (17, 18) (Fig. 1c) was used for the 2 MRI sessions.

Breathing training session with AV biofeedback

Before MRI sessions, each patient participated in a breathing training session with AV biofeedback (no imaging performed) to allow them to become familiar the AV biofeedback breathing guidance and obtain a guiding wave to be used in 2 MRI sessions.

This session was to allow the patient to practice their breathing for approximately 30 minutes to 1 hour, which included the acquisition of up to 3 guiding waves and breathing practices. Once a guiding wave was acquired, patients were guided by AV biofeedback for 5 to 10 minutes in a practice session. After each breathing practice, on the basis of a discussion with the patient, the displacement and period of the guiding wave was modified to make it more comfortable before allowing the patient to practice with the modified guiding wave. This was repeated 2 to 3 times, until the patients were comfortable using the guiding wave. At the end of a breathing training session, the guiding wave the patient was most comfortable with was chosen and used for the subsequent MRI sessions.

Magnetic resonance imaging with AV biofeedback

Two-dimensional (2D) coronal and sagittal cine-MR images were obtained in a 3T MRI (Skyra, Siemens Healthcare, Erlangen, Germany). For thoracic imaging, a true-FISP (true fast imaging with steady-state free precession) MR pulse sequence was used to acquire 512 images per 2D cine-MR image every 308 ms. Typical MR imaging parameters were repetition time/echo time = 38/13 ms, flip angle = 45°, field of view = 380 × 380 mm^2, pixel size = 1.48 × 1.48 mm^2, slice thickness = 4 mm, bandwidth = 1500 Hz, and image matrix = 256 × 256.

Coronal and sagittal images were obtained at different positions (center of the tumor region) and times (coronal followed by sagittal) with (*1*) free breathing (FB) and (*2*) AV biofeedback across the first and second MRI sessions. Hence, tumor motion varied between coronal and sagittal image datasets. At the beginning of an MRI session with AV biofeedback, the guiding wave was loaded to display on a patient screen (Fig. 1b). Eight datasets per patient (2 image datasets [coronal and sagittal] × 2 breathing types [FB and AV]) were obtained from 2 MRI sessions; however, only 4 datasets were obtained from the first MRI session of patients 5 and 8, because the patients withdrew from study before the second MRI session.

Tumor auto-segmentation

Tumor motion was directly measured from cine-MR images through auto-segmentation, to consider the changes in displacement and shape. Auto-segmentation was performed in the following steps. (*1*) A single seed point on the tumor region was manually chosen on the first image of each dataset, and an arbitrary image pixel matrix (ie, 9 × 9) surrounding the single seed point was chosen (but a smaller [or bigger] matrix size can be used, depending on tumor size). (*2*) For the range of image intensity (threshold), an average of 3 minimum and maximum pixel values of the arbitrary image pixel matrix was computed to filter tumor image intensity within the threshold. (*3*) Otsu's method (25) was used to convert a grayscale image to a binary image in normalized image intensity value that lies in the range [0, 1]. (*4*) The tumor was segmented by a region-growing algorithm (26) with the seed point on the binary image. The centroid of tumor motion was calculated using the mean of row and column positions where binary pixel values were equal to 1. In the next image, the tumor was segmented using the present centroid as a seed point until all binary images were segmented. All segmented tumors were visually inspected to assess auto-segmentation. If an abrupt motion occurred, a new seed point would be chosen again, but this did not happen for all datasets.

An in-house tumor auto-segmentation was implemented in MATLAB version 8.2 (The MathWorks, Natick, MA) and used for 2D coronal and sagittal cine-MR image datasets.

Tumor motion consistency

For the impact of the use of AV biofeedback, tumor motion consistency was investigated in (*1*) intrafraction tumor motion in each dataset and (*2*) interfraction tumor motion over 2 datasets from the first and second MRI sessions. For intrafraction tumor motion consistency, the centroid of tumor motion was separated into individual cycles of a peak to peak (or a trough to trough), excluding incomplete data, and the root mean square error (RMSE) of a cycle to cycle in displacement (19) was computed while comparing the average cycle of the individual cycles with each individual cycle. The RMSE in period was also computed from each individual cycle.

For interfraction tumor motion consistency, the RMSE of a session to session in displacement and period was computed by comparing 2 average cycles of the 2 datasets. To match tumor motion variability to outlier motion, each segmented tumor was accumulated on a pixel-by-pixel basis over the path of all segmented tumors in each dataset and then over 2 datasets at their center. Then the value of the pixels (frequency), how many times the tumor passed, and the number of pixels (distribution) where the tumor passed more than once were quantified. For example, the frequency of all the pixel values can be the same as the number of segmented tumors if no tumor motion and shape changes occur. However, a widespread distribution in various frequencies, directly connected to treatment margins, can be expected if a large baseline shift and displacement change of tumor motion occurs (9, 27). To evaluate outlier motion caused by baseline shifts and irregular breathing, we computed the ratio of the distribution in which the tumor was found 5% or more of the time to the total distribution encompassed by the tumor motion. This ratio, referred to henceforth as the *outlier motion ratio*, was computed for all of the patient datasets for FB and AV. Quantitative statistical comparison between AV biofeedback and FB was determined using the RMSE in displacement and period for intrafraction tumor motion consistency, and the RMSE in displacement and period and the outlier motion ratio for interfraction tumor motion consistency, using a paired Student *t* test.

Results

Figure 2 shows the 9 lung tumors delineated by auto-segmentation on coronal and sagittal cine-MR images. Segmented tumors at the end of exhalation and inhalation were chosen for each patient.

The location of the identified tumors (blue line) varied across patients: (*1*) 4 tumors (patients 3, 4, 5, and 7) were on the left lung, and 5 (patients 1, 2, 6, 8, and 9) were on the right lung; (*2*) 5 (patients 1, 5, 7, 8, and 9) were on the upper lung, and 4 (patients 2, 3, 4, and 6) were on the middle lung; and (*3*) 3 (patients 1, 4, and 6) were isolated from organs, but the other 6 (patients 2, 3, 5, 7, 8, and 9) were connected to (or between) organs. In addition, tumor shape varied on different coronal and sagittal image orientations: (*1*) 2 (patients 1 and 4) were mostly the same shape on both image orientations, but the other 7 (patients 2, 3, 5, 6, 7, 8, and 9) were considerably different between image orientations. All tumors moved in the direction of respiratory motion, apart from patient 2, in whom the tumor attached to the chest wall moved superiorly during expiration.

Intrafraction tumor motion consistency

Figure 3 shows a comparison of tumor motion between FB and AV biofeedback. Four superior–inferior tumor displacements indicate the different combinations of breathing type and MRI session in patients 4 and 6.

The tumor of patient 4 moved in a small range of ±0.5 cm, whereas a large range of ±3 cm was found in patient 6. In patient 4, the baseline of tumor displacement continuously drifted over the entire FB session 1, and the tumor displacement of FB session 2 was more regular but smaller, whereas the regularity of tumor displacement was improved over AV biofeedback sessions. In patient 6, regular tumor displacement was found in the AV biofeedback sessions, compared with irregular tumor displacement in both FB sessions due to a drift, stable and breath hold.

Table 1 shows the intrafraction tumor motion consistency results with FB and AV biofeedback in the RMSE of displacement and period.

The RMSE displacement of intrafraction tumor motion varied with AV biofeedback between 0.02 and 0.45 cm, but it was larger for FB, with RMSE displacement between 0.03 and 0.99 cm. Only 2 patients with AV biofeedback had more than 0.1 cm in RMSE displacement, compared with 4 patients with FB. In addition, the RMSE period with AV biofeedback was between 0.16 s and 1.02 s, which were smaller than FB, with an RMSE period between 0.26 s and 4.93 s. Intrafraction RMSE values were significantly reduced by 34% in displacement (P=.019) and by 73% in period (P<.001) when AV biofeedback was used, whereas there was no difference in mean displacement and period with FB and AV biofeedback.

Interfraction tumor motion consistency

Table 2 shows the interfraction tumor motion consistency results with FB and AV biofeedback in the RMSE of displacement and outlier motion ratio. The interfraction tumor motion consistency in period was increased by 74% in period (P=.005).

The RMSE displacement of interfraction tumor motion varied with AV biofeedback at 0.22 cm, but it was larger with FB at 0.44 cm. Only 1 patient with AV biofeedback had more than 0.1 cm in RMSE displacement, compared with 2 patients with FB. In addition, the outlier motion ratio with AV biofeedback was between 24% and 42%, and it was also larger with FB, between 31%

and 50%. Interfraction variation of RMSE using AV biofeedback was reduced by 42% (P=.046) in displacement, and the outlier motion ratio was also decreased by 21% (P<.001).

Figure 4 shows the distribution of tumor motion and the outlier motion for patients 4 and 6 with FB and with AV biofeedback. A widespread outlier motion in the same color bar scale indicates more variation of interfraction tumor motion. The results of sagittal image datasets for Patients 4 and 6 are shown in Figure e1 (supplementary material).

A widespread outlier motion with FB was found, due to irregular tumor displacement (see FB sessions in Fig. 3) in both patients, whereas the comparatively regular tumor displacement (see AV biofeedback sessions in Fig. 3) resulted in a smaller outlier motion with AV biofeedback. Subsequently, the color bar scale of outlier motion was smaller with AV biofeedback in both patients.

Discussion

Medical imaging and radiation treatment in thoracic and abdominal regions often requires tumor motion management, owing to the variability of tumor motion pattern both intrafractionally and interfractionally. In this work, we introduced AV biofeedback that uses the same guiding wave from the breathing training session customized for each patient in displacement and period across repeated MRI sessions, to reduce intra- and interfraction tumor motion consistency. Using AV biofeedback, we demonstrated improvement of tumor motion consistency in intrafraction displacement and period and interfraction displacement and period, and outlier motion while using the segmented tumor directly measured on coronal and sagittal cine-MR images.

Respiratory-induced thoracic and abdominal tumor motion varies with tumor size, location, and patients (28), and this study also demonstrated independent tumor locations and sizes through tumor auto-segmentation. Tumor motion also varied in an MRI session and across 2 MRI sessions, but it was improved with AV biofeedback compared with FB. In previous studies, intrafraction regularity in displacement was improved by more than 50% (external abdomen) (19) and 38% (internal diaphragm) (17). This study demonstrated that the intrafraction tumor motion consistency of all patients with AV biofeedback in Table 1 was improved by 34% and 73% in displacement and period, respectively. In addition, interfraction tumor motion consistency in Table 2 was improved by 42% in displacement and by 74% in period. Then, those significant improvements resulted in 21% reduction of the outlier motion ratio, directly linked to the minimization of the disagreement between planning and treatment, resulting in more dose delivered to the tumor itself and less dose to the surrounding healthy tissue (6, 7, 8, 29). Consequently, AV biofeedback can be applicable for respiratory motion management techniques, such as respiratory gating (10), training (11), and breath-hold (12), owing to tumor motion consistency.

The external respiratory signal can be replaced with any respiratory signals, such as ANZAI (AZ-733V, Anzai Medical Corporation, Tokyo, Japan) (30) and Bellows-belt (31), and internal respiratory signals, such as MR navigator (32) and electromagnetic transponder (33). In addition, tumor motion from MR images could be used as the respiratory signal input for AV biofeedback. If tumor motion using faster imaging (34) in MRI integrated with a radiation therapy system (35, 36) is used for lung tumor motion management, real-time tumor deformation (37) can be used for image-guided AV biofeedback.

One of the limitations of the present study was that the interfraction changes were determined using only 2 MRI sessions, 1 before and the other in the middle of treatment. Tumor segmentation included manual work to set a seed point on an MR image and manual validation of the segmentation method.

We also skipped 3 to 5 images at the beginning of datasets owing to the MR images being too bright. This study did not consider tumor deformation or out-of-plane motion. For better quantification of deformed tumor motion compared with only rigid motion, deformable image registration could be used, as well as 3-dimensional tumor motion using 3-dimensional MRI (18).

Conclusions

This was the first study to directly evaluate the impact of audiovisual biofeedback on lung tumor motion in cine-MRI. By using AV biofeedback, interfraction and intrafraction tumor motion consistency was improved across 2 MRI sessions, spaced several weeks apart. Audiovisual biofeedback led to a 34% and 73% improvement of tumor motion consistency in intrafraction displacement and period, respectively. Audiovisual biofeedback also led to an improvement of 42% and 74% and 21% in interfraction displacement and period and outlier motion ratio, respectively. These results demonstrate that AV biofeedback can facilitate consistent lung tumor motion, which could be a desirable technique for achieving more accurate medical imaging and radiation therapy procedures.

References

1. Hugo G, Vargas C, Liang J, et al. Changes in the respiratory pattern during radiotherapy for cancer in the lung. Radiother Oncol 2006;78: 326-331.

2. Smith RP, Bloch P, Harris EE, et al. Analysis of interfraction and intrafraction variation during tangential breast irradiation with an electronic portal imaging device. Int J Radiat Oncol Biol Phys 2005; 62:373-378.

3. Juhler Nøttrup T, Korreman SS, Pedersen AN, et al. Intra-and interfraction breathing variations during curative radiotherapy for lung cancer. Radiother Oncol 2007;84:40-48.

4. Liu HH, Balter P, Tutt T, et al. Assessing respiration-induced tumor motion and internal target volume using four-dimensional computed tomography for radiotherapy of lung cancer. Int J Radiat Oncol Biol Phys 2007;68:531-540.

5. Matsugi K, Narita Y, Sawada A, et al. Measurement of interfraction variations in position and size of target volumes in stereotactic body radiotherapy for lung cancer. Int J Radiat Oncol Biol Phys 2009;75: 543-548.

6. Yamamoto T, Langner U, Loo BW Jr., et al. Retrospective analysis of artifacts in four-dimensional CT images of 50 abdominal and thoracic radiotherapy patients. Int J Radiat Oncol Biol Phys 2008;72:1250- 1258.

7. Balter JM, Ten Haken RK, Lawrence TS, et al. Uncertainties in CTbased radiation therapy treatment planning associated with patient breathing. Int J Radiat Oncol Biol Phys 1996;36:167-174.

8. Ge J, Santanam L, Noel C, et al. Planning 4-dimensional computed tomography (4DCT) cannot adequately represent daily intrafractional motion of abdominal tumors. Int J Radiat Oncol Biol Phys 2013;85: 999-1005.

9. Keall PJ, Mageras GS, Balter JM, et al. The management of respiratory motion in radiation oncology report of AAPM Task Group 76. Med Phys 2006;33:3874-3900.

10. Kini VR, Vedam SS, Keall PJ, et al. Patient training in respiratorygated radiotherapy. Med Dosim 2003;28:7-11.

11. George R, Vedam S, Chung T, et al. The application of the sinusoidal model to lung cancer patient respiratory motion. Med Phys 2005;32: 2850-2861.

12. Murphy MJ, Martin D, Whyte R, et al. The effectiveness of breathholding to stabilize lung and pancreas tumors during radiosurgery. Int J Radiat Oncol Biol Phys 2002;53:475-482.

13. Ge J, Santanam L, Yang D, et al. Accuracy and consistency of respiratory gating in abdominal cancer patients. Int J Radiat Oncol Biol Phys 2013;85:854-861.

14. Shah AP, Kupelian PA, Waghorn BJ, et al. Real-time tumor tracking in the lung using an electromagnetic tracking system. Int J Radiat Oncol Biol Phys 2013;86:477-483.

15. Hoogeman M, Pre´vost JB, Nuyttens J, et al. Clinical accuracy of the respiratory tumor tracking system of the cyberknife: Assessment by analysis of log files. Int J Radiat Oncol Biol Phys 2009;74:297-303.

16. George R, Chung TD, Vedam SS, et al. Audio-visual biofeedback for respiratory-gated radiotherapy: Impact of audio instruction and audiovisual biofeedback on respiratory-gated radiotherapy. Int J Radiat Oncol Biol Phys 2006;65:924-933.

17. Kim T, Pollock S, Lee D, et al. Audiovisual biofeedback improves diaphragm motion reproducibility in MRI. Med Phys 2012;39:6921- 6928.

18. Lee D, Greer P, Arm J, et al. Audiovisual biofeedback improves image quality and reduces scan time for respiratory-gated 3D MRI. J Phys Conf Ser 2014;489:012033.

19. Venkat RB, Sawant A, Suh Y, et al. Development and preliminary evaluation of a prototype audiovisual biofeedback device incorporating a patient-specific guiding waveform. Phys Med Biol 2008;53: N197.

20. Steel H, Pollock S, Lee D, et al. The internal-external respiratory motion correlation is unaffected by audiovisual biofeedback. Australas Phys Eng Sci Med 2014;37:97-102.

21. Lu W, Neuner GA, George R, et al. Audio-visual biofeedback does not improve the reliability of target delineation using maximum intensity projection in 4-dimensional computed tomography radiation therapy planning. Int J Radiat Oncol Biol Phys 2014;88:229-235.

22. Keall P, Yang J, Yamamoto T, et al. SU-D-17A-04: The impact of audiovisual biofeedback on image quality during 4D functional and anatomic imaging: Results of a prospective clinical trial. Med Phys 2014;41:117.

23. Pollock S, Lee D, Kim T, et al. SU-E-J-142: Respiratory guidance for lung cancer patients: An investigation of audiovisual biofeedback training and effectiveness. Med Phys 2013;40:183.

24. Fitzpatrick MJ, Starkschall G, Antolak JA, et al. Displacement-based binning of time-dependent computed tomography image data sets. Med Phys 2006;33:235-246.

25. Otsu N. A threshold selection method from gray-level histograms. Automatica 1975;11:23-27.

26. Gonzalez RC, Woods RE, Eddins SL. Digital Image Processing Using MATLAB. Upper Saddle River, NJ: Pearson Prentice Hall; 2004.

27. Akino Y, Oh RJ, Masai N, et al. Evaluation of potential internal target volume of liver tumors using cine-MRI. Med Phys 2014;41:111704.

28. Stevens CW, Munden RF, Forster KM, et al. Respiratory-driven lung tumor motion is independent of tumor size, tumor location, and pulmonary function. Int J Radiat Oncol Biol Phys 2001;51:62-68.

29. Van Herk M. Errors and margins in radiotherapy. Semin Radiat Oncol 2004;14:52-64.

30. Li XA, Stepaniak C, Gore E. Technical and dosimetric aspects of respiratory gating using a pressure-sensor motion monitoring system. Med Phys 2006;33:145-154.

31. Santelli C, Nezafat R, Goddu B, et al. Respiratory bellows revisited for motion compensation: Preliminary experience for cardiovascular MR. Magn Reson Med 2011;65:1097-1102.

32. Spincemaille P, Nguyen TD, Prince MR, et al. Kalman filtering for real-time navigator processing. Magn Reson Med 2008;60: 158-168.

33. Keall PJ, Colvill E, O'Brien R, et al. The first clinical implementation of electromagnetic transponder-guided MLC tracking. Med Phys 2014;41:020702.

34. Lee D, Pollock S, Whelan B, et al. Dynamic keyhole: A novel method to improve MR images in the presence of respiratory motion for realtime MRI. Med Phys 2014;41:072304.

35. Raaymakers B, Lagendijk J, Overweg J, et al. Integrating a 1.5 T MRI scanner with a 6 MV accelerator: Proof of concept. Phys Med Biol 2009;54:N229.

36. Kolling S, Oborn B, Keall P. Impact of the MLC on the MRI field distortion of a prototype MRI-linac. Med Phys 2013;40: 121705.

37. Ge Y, O'Brien RT, Shieh CC, et al. Toward the development of intrafraction tumor deformation tracking using a dynamic multi-leaf collimator. Med Phys 2014;41:061703.

Table 1 Results for intrafraction tumor motion consistency in RMSE of displacement and period

Patient	RMSE displacement (cm)				RMSE period (s)			
	FB Cor	FB Sag	AV Cor	AV Sag	FB Cor	FB Sag	AV Cor	AV Sag
P1								
S1	0.25	0.14	0.16	0.10	1.22	0.53	0.66	0.32
S2	0.08	0.07	0.14	0.12	0.54	0.32	0.33	0.36
P2								
S1	0.07	0.04	0.07	0.06	0.72	0.95	0.49	1.02
S2	0.07	0.05	0.09	0.04	0.73	0.76	0.24	0.38
P3								
S1	0.07	0.06	0.06	0.07	0.50	0.38	0.38	0.53
S2	0.06	0.09	0.07	0.05	0.26	0.50	0.22	0.28
P4								
S1	0.18	0.05	0.05	0.03	1.38	1.38	0.22	0.23
S2	0.04	0.04	0.04	0.03	0.49	0.46	0.21	0.16
P5								
S1	0.05	0.08	0.04	0.03	0.47	0.32	0.36	0.22
P6								
S1	0.50	0.29	0.23	0.18	1.38	0.96	0.19	0.28
S2	0.99	0.51	0.45	0.32	1.83	0.48	0.36	0.28

Patient	RMSE displacement (cm)				RMSE period (s)			
	FB Cor	FB Sag	AV Cor	AV Sag	FB Cor	FB Sag	AV Cor	AV Sag
P7								
S1	0.12	0.08	0.08	0.05	1.23	2.11	0.25	0.26
S2	0.13	0.16	0.04	0.08	1.33	1.70	0.23	0.26
P8								
S1	0.07	0.03	0.03	0.03	1.42	4.93	0.23	0.33
P9								
S1	0.03	0.01	0.03	0.02	1.04	0.53	0.24	0.18
S2	0.03	0.04	0.03	0.03	1.06	0.67	0.18	0.22
Average	0.20	0.13	0.12	0.09	0.98	1.34	0.30	0.39
P[*]	.019				<.001			

Abbreviations: AV = audiovisual; Cor = coronal; FB = free breathing; P = patient; RMSE = root mean square error; S = MRI session; Sa = sagittal.
A smaller number of RMSE indicates more consistent tumor motion.

* Paired Student *t* test between FB and AV biofeedback (coronal and sagittal together).

Table 2. Results for interfraction tumor motion consistency in RMSE of displacement and outlier motion ratio

Patient	RMSE displacement (cm)				Outlier motion ratio (%)			
	FB Cor	FB Sag	AV Cor	AV Sag	FB Cor	FB Sag	AV Cor	AV Sag
P1	0.07	0.05	0.06	0.03	40	39	35	31
P2	0.13	0.09	0.06	0.06	30	31	29	23
P3	0.05	0.05	0.02	0.05	32	40	26	42
P4	0.03	0.03	0.02	0.02	50	38	25	24
P6	0.44	0.21	0.22	0.11	35	42	25	29
P7	0.06	0.03	0.05	0.03	39	36	33	35
P9	0.01	0.01	0.01	0.01	36	42	33	29
Average	0.11	0.07	0.06	0.04	37	38	29	30
P	.046				<.001			

Abbreviations as in Table 1.
A smaller number indicates more consistent tumor motion.

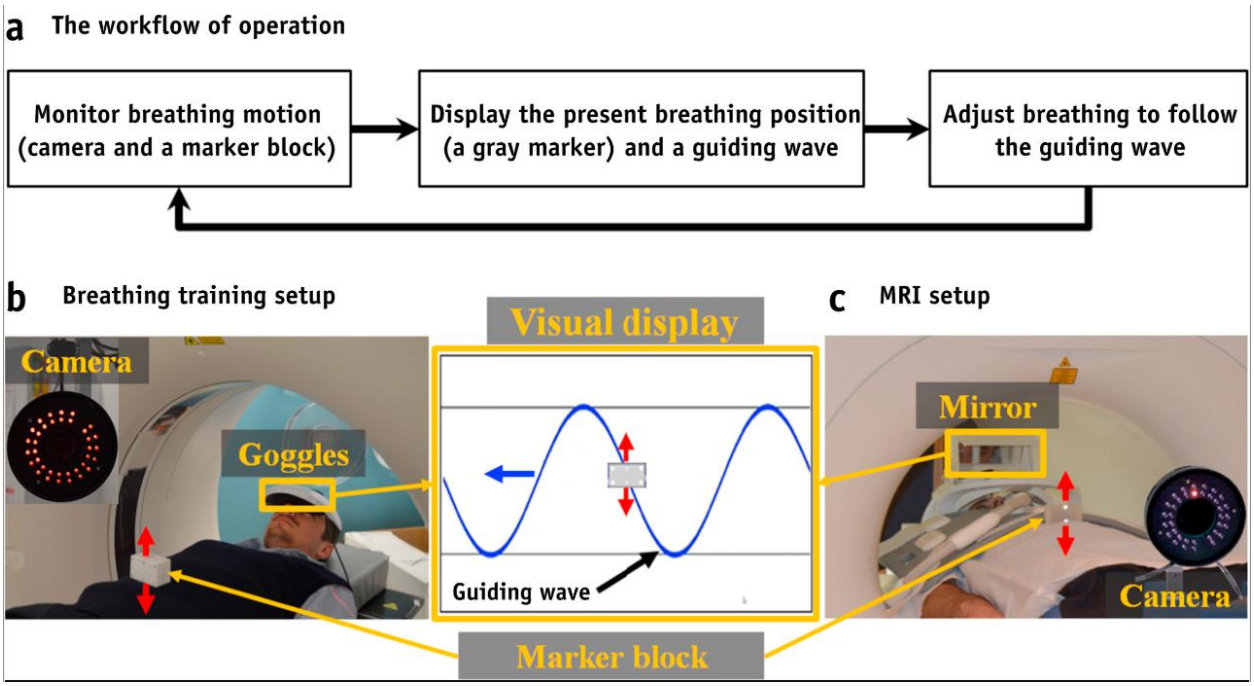

Fig. 1. Workflow of operation and experimental setups of audiovisual biofeedback. (a) Workflow of operation, (b) breathing training setup for a breathing training session, and (c) magnetic resonance imaging (MRI) setup for 2 MRI sessions.

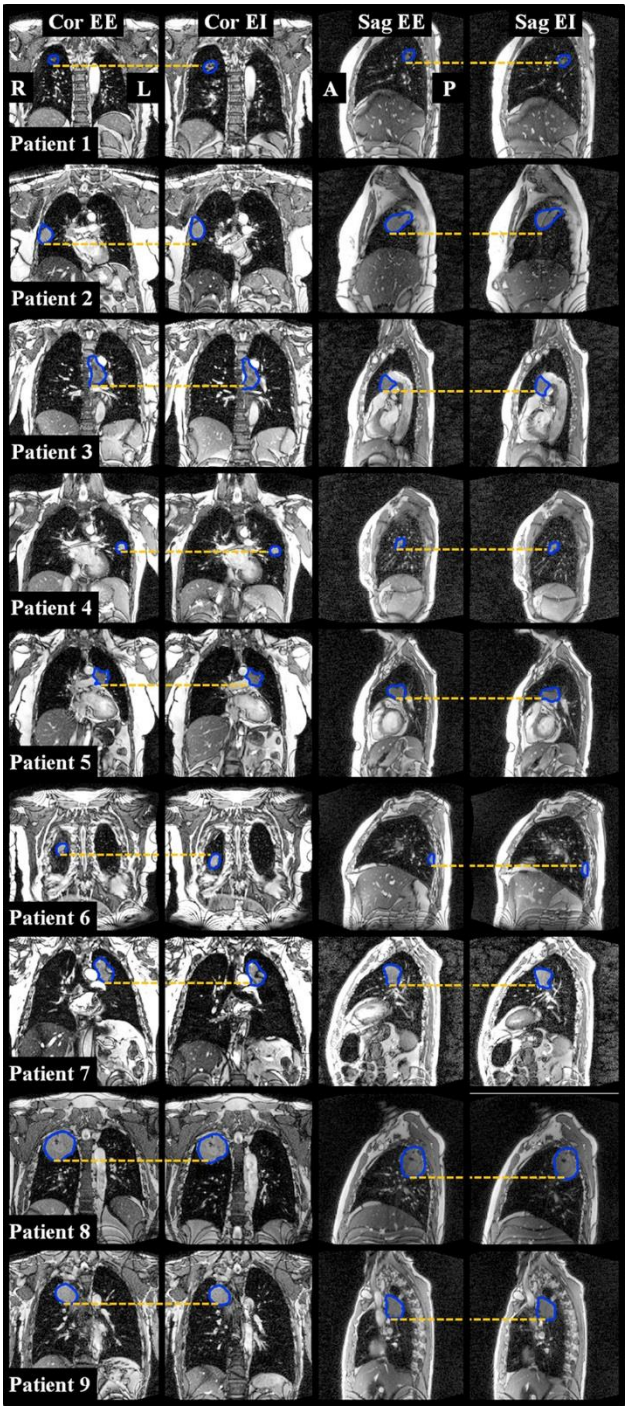

Fig. 2. Tumor delineation (blue line) of 9 lung cancer patients. Segmented tumors at end of exhalation (EE) and end of inhalation (EI) were chosen for each patient, and an orange dotted line highlights the changes in tumor displacement.

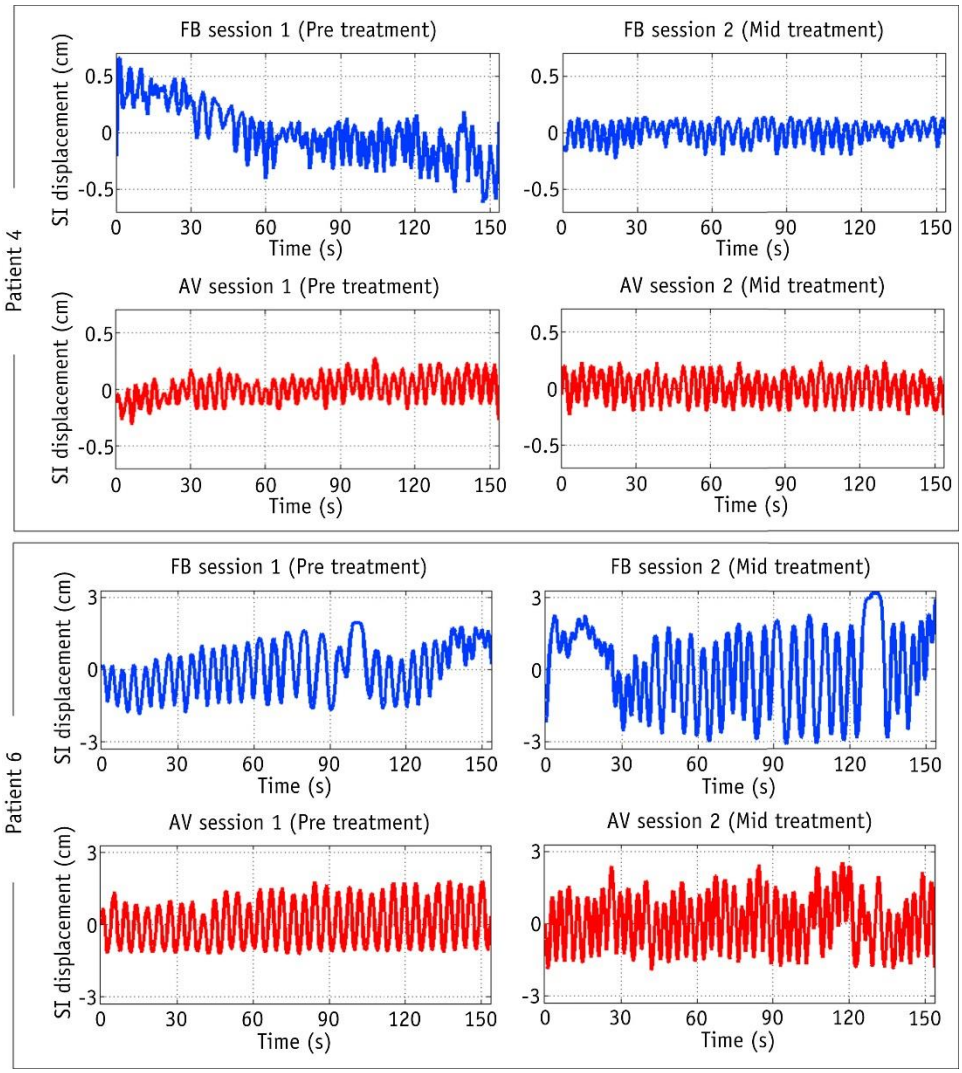

Fig. 3. Superior–inferior tumor displacement (cm) of patients 4 and 6 between free breathing (FB) and audiovisual biofeedback (AV) measured from coronal image datasets and organized by breathing type and magnetic resonance imaging session. Extreme displacements were either a function of continuous drift with FB in patient 4 or a drift, stable and breath hold with FB in patient 6.

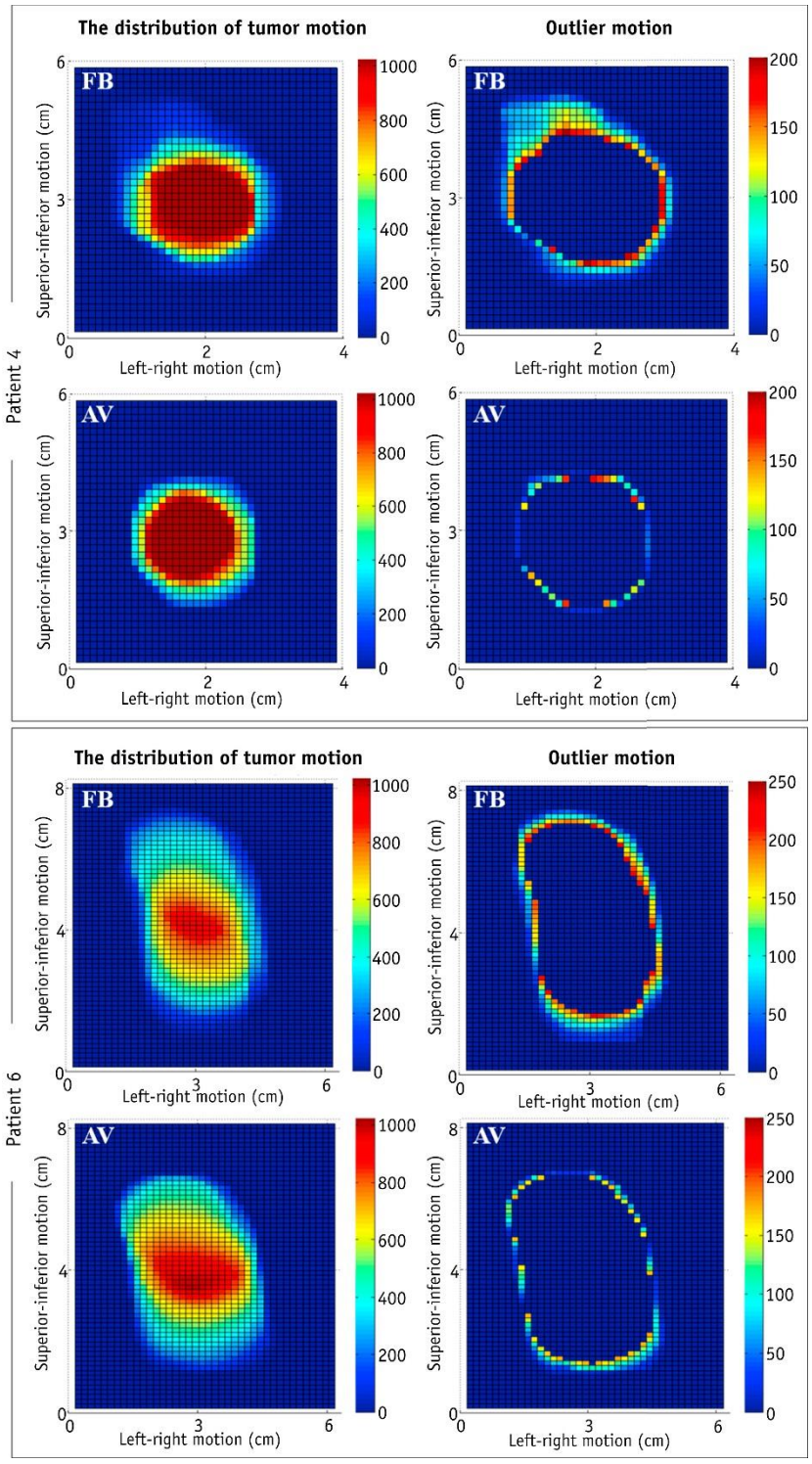

Fig. 4. Distribution of tumor motion and the outlier motion measured from coronal image datasets for patients 4 and 6. Color bar scale indicates the ratio of the distribution of tumor motion.